HHS Public Access

Author manuscript

Bone. Author manuscript; available in PMC 2018 October 01.

Published in final edited form as:

Bone. 2017 October ; 103: 159–167. doi:10.1016/j.bone.2017.06.027.

PARATHYROID HORMONE INHIBITS NOTCH SIGNALING IN OSTEOBLASTS AND OSTEOCYTES

Stefano Zanotti and **Ernesto Canalis**

Departments of Orthopaedic Surgery and Medicine, and the UConn Musculoskeletal Institute, UConn Health, Farmington, CT 06030

Abstract

Parathyroid hormone (PTH) and Notch receptors regulate bone formation by governing the function of osteoblastic cells. To determine whether PTH interacts with Notch signaling as a way to control osteoblast function, we tested the effects of PTH on Notch activity in osteoblast- and osteocyte-enriched cultures. Notch signaling was activated in osteoblast-enriched cells from wild-type C57BL/6J mice following exposure to the Notch ligand Delta-like (Dll)1 or by the transient transfection of the Notch intracellular domain (NICD), the transcriptionally active fragment of Notch1. To induce Notch signaling in osteocyte-enriched cultures, a murine model of *Notch2* gain-of-function was used. PTH opposed the stimulatory effects of Dll1 on *Hey1*, *Hey2* and *HeyL* mRNA levels in osteoblast-enriched cells and suppressed the expression of selected Notch target genes in osteocyte-enriched cultures, either under basal conditions or in the context of *Notch2* gain-of-function. Induction of Notch signaling in osteocytes did not alter the inhibitory effect of PTH on *Sost* expression, but reduced the stimulation of *Tnfsf11* mRNA levels by PTH. In agreement with these *in vitro* observations, male mice administered with PTH displayed suppressed *Hey1* and *HeyL* expression in parietal bones. Transactivation experiments with a Notch reporter construct and electrophoretic mobility shift assays in osteoblast-enriched cells suggest that PTH acts by decreasing the capacity of Rbpjκ to bind to DNA. In conclusion, downregulation of Notch in osteoblasts and osteocytes may represent a mechanism contributing to the anabolic effects of PTH in bone.

Keywords

PTH; Notch; Rbpjκ; osteoblast; osteocyte

1. INTRODUCTION

Bone remodeling is the process whereby the coordinated activities of osteoblasts and osteoclasts preserve skeletal integrity and contribute to the regulation of mineral metabolism

Address correspondence to: Stefano Zanotti, Ph.D., Department of Orthopaedic Surgery, UConn Health, Farmington, CT, 06030-5456, USA, Tel: (860) 679-2355; Fax: (860) 679-1474; zanotti@uchc.edu.

[1]. Bone-forming osteoblasts derive from mesenchymal precursors and can mature further into quiescent bone lining cells or become embedded in the mineralized matrix as osteocytes. These are terminally differentiated cells that confer the skeleton the ability of sensing and adapting to mechanical stimuli [2]. Osteoblasts and osteocytes secrete receptor activator of nuclear factor-Kappa B-ligand (Rankl), a peptide encoded by *Tnfsf11* that stimulates the formation of bone-resorbing osteoclasts. As a consequence, osteoblasts and osteocytes have the capacity to control bone resorption [3]. An attribute that distinguishes osteocytes from osteoblasts is the ability to express high levels of *Dmp1* and *Sost*, the genes encoding for dentin matrix protein 1 and sclerostin, respectively [4–6]. The latter is a secreted molecule that inhibits osteoblast differentiation by suppressing Wnt/β-catenin signaling [7].

Parathyroid hormone (PTH) is an 84-amino acid peptide that regulates the function of osteoblasts and osteocytes, and is secreted by the parathyroid gland in response to changes in the concentration of extracellular calcium [8–10]. PTH enhances bone formation by a variety of mechanisms, including direct effects on the osteoblast, the induction of insulin-like growth factor I and possibly the suppression of *Sost* [11, 12]. However, neither changes in *Sost* expression nor the presence of osteocytic/osteoblastic β-catenin are required for the anabolic actions of PTH suggesting the involvement of other mechanisms [13, 14]. PTH also enhances bone resorption by inducing *Tnfsf11* in osteoblasts and osteocytes [15, 16]. Direct stimulation of osteoblast function by PTH is mediated primarily by the activation of the cAMP/protein kinase A and the mitogen activated protein kinases (MAPK) [17]. The intracellular mechanisms of PTH action in osteocytes are not well understood, in part due to the lack of a suitable model for the study of osteocyte function *in vitro*.

The four Notch receptors and their cognate ligands of the Delta-like (Dll) and Jagged (Jag) families are transmembrane proteins that mediate communication between adjacent cells. Activation of Notch receptors occurs following their cleavage and release of the intracellular domain (NICD), which translocates to the nucleus, associates with a DNA binding factor termed recombination signal binding protein for immunoglobulin kappa J region (Rbpj)κ, and induces gene expression [18]. Rbpjκ is the murine ortholog of core binding factor-1/suppressor of hairless/Lag-1 (CSL). Classic target genes of Rbpjκ-mediated Notch signaling are *Hes1*, *Hes5* and *Hes7* as well as *Hey1*, *Hey2* and *HeyL* [19]. Notch1 and Notch2 regulate bone remodeling, and their actions are determined by the degree of osteoblast maturity [20]. In contrast to the bone anabolic effects of PTH, induction of Notch1 in mesenchymal precursor cells and mature osteoblasts suppresses cell differentiation and trabecular bone formation, and Notch2 exerts similar inhibitory effects on osteoblast function [21–26]. Conversely, activation of Notch1 in osteocytes induces osteoprotegerin and suppresses sclerostin, leading to an osteopetrotic phenotype [23, 27].

PTH is known to induce the Notch ligand Jag1 in osteoblasts and potentially activate Notch signaling, and the effects of PTH on osteoblast differentiation were opposed by γ-secretase inhibitors, suggesting that Notch mediates selected actions of PTH in osteoblasts [28, 29]. However, γ-secretase inhibitors have nearly 100 substrates and therefore are not specific to the activation Notch signaling [30]. In addition, PTH exposure and Notch induction have opposite consequences on bone formation and osteoblast activity. These apparently

contradictory observations could be explained by additional interactions between PTH and Notch in osteoblastic cells.

In the present study, we tested the effects of PTH on Notch signaling in osteoblasts from wild-type mice and osteocytes from a recently described murine model of *Notch2* gain-of-function [25]. These experiments were complemented by *in vivo* work to determine the impact of PTH on Notch signaling in bone tissue of wild-type mice.

2. MATERIALS AND METHODS

2.1 Mice

Wild-type C57BL/6J mice (Jackson Laboratory, Bar Harbor, ME) were used as a source of primary osteoblastic cells for *in vitro* experiments. To test the effects of PTH on Notch signaling in bone *in vivo*, 7 week old wild-type male mice were injected subcutaneously with 80 μg/Kg of the PTH amino terminal fragment 1–34 (Sigma-Aldrich, St. Louis, MO) dissolved in phosphate buffered saline (PBS). Mice injected with an equal volume of PBS served as controls. Parietal bones were harvested at sacrifice, frozen in liquid nitrogen and stored at −80°C.

To achieve *Notch2* gain-of-function, mice harboring a point mutation in exon 34 of the *Notch2* locus were generated by homologous recombination, as described [25]. A 6955C>T mutation was introduced creating a stop codon leading to the translation of a truncated protein lacking the proline-, glutamic acid-, serine- and threonine-rich (PEST) domain, making it resistant to degradation and resulting in a *Notch2* gain-of-function [20]. The homologous mutation in humans is associated with Hajdu Cheney syndrome (HCS), and the model was named *Notch2HCS*. Heterozygous *Notch2HCS* mice were bred to wild-type mice to create experimental heterozygous *Notch2HCS* mice and wild-type littermate controls in a 129SvJ/C57BL/6J genetic background. The presence of the *Notch2HCS* allele was determined in tail DNA extracts by polymerase chain reaction (PCR) using forward 5′-CCCTTCTCTCTGTGCGGTAG-3′ and reverse 5′-CTCAGAGCCAAAGCCTCACTG-3′ primers (both from Integrated DNA Technologies; IDT, Coralville, IA). Experimental protocols were approved by the Institutional Animal Care and Use Committees of Saint Francis Hospital and Medical Center (Hartford, CT) and of UConn Health.

2.2 Osteoblast-enriched Cultures

Parietal bones of 3 to 5 day old wild-type mice were digested at 37°C with type-II collagenase from *Clostridium histolyticum* (Worthington Biochemical Corp., Lakewood, NJ) and treated with N-α-tosyl-L-lysyl-chloromethylketone hydrochloride (TLCK; Calbiochem, La Jolla, CA). Five sequential digestions were carried out and cells extracted from the last 3 digestions were pooled and cultured in Dulbecco's modified Eagle's medium (DMEM) supplemented with non-essential amino acids (both from Life Technologies, Grand Island, NY), 20 mM HEPES, 100 μg/ml ascorbic acid (both from Sigma-Aldrich) and heat-inactivated 10% fetal bovine serum (FBS, Atlanta Biologicals, Inc., Atlanta, GA), in a humidified 5% CO_2 incubator at 37°C, as described [31]. To activate Notch receptors, osteoblast-enriched cells were trypsinized and seeded at a density of 22,000 cells/cm^2 on

culture plates coated with a Dll1-IgG_{2A} fragment crystallizable (Fc) recombinant fusion protein 125 ng/cm^2 (R&D Systems, Minneapolis, MN), and cultured for 24 h. Parallel cultures on an equimolar amount of bovine serum albumin (BSA) served to establish basal levels of Notch signaling, as BSA is considered to be a suitable control for recombinant Fc fusion proteins [32]. To prevent the effects of serum-derived factors, cultures were serum deprived 24 h prior to the addition of PTH at 10 nM for 6 h. No negative consequences are observed on osteoblast viability after a 24 h serum deprivation [33].

2.3 Osteocyte-enriched Cultures

Femurs from 6 or 7 week old wild-type or *Notch2HCS* mice were collected after sacrifice, surrounding tissues dissected, the proximal epiphysis excised, and the bone marrow removed by centrifugation. The distal epiphysis was removed, and to release the endosteal and periosteal cellular layers, the femoral fragments were sequentially exposed for 20 min periods at 37°C to type-II collagenase pretreated with TLCK 17 μg/ml or EDTA 5 mM (Life Technologies), as stated in figure legends. In an initial experiment, cells were obtained after 5 sequential collagenase/EDTA digestions as described in previous publications [34]. Cells from each digestion step, and the remaining bone fragments were collected and analyzed for gene expression. Subsequently, osteocyte-enriched bone fragments were obtained after a single collagenase and an EDTA digestion, and either analyzed or cultured individually in DMEM supplemented with nonessential amino acids, 100 μg/ml ascorbic acid, and heat-inactivated 10% FBS for 4 days in a humidified 5% CO_2 incubator at 37°C [35, 36]. Cultures were serum deprived for 24 h prior to treatment with PTH 10 nM or vehicle for 6 h, and femoral fragments frozen in liquid nitrogen and stored at −80°C.

RNA Integrity and Quantitative Reverse Transcription-PCR (qRT-PCR)—Total RNA was extracted from osteoblast-enriched cells and from cellular fractions obtained after collagenase/EDTA digestions of femoral fragments with an RNeasy kit (Qiagen, Valencia, CA). Osteocyte-enriched femoral fragments or parietal bones were homogenized prior to chloroform/phenol extraction of total RNA with the micro RNeasy kit (Qiagen). Integrity of RNA preparations was assessed by microfluidic electrophoresis on an Experion system (Bio-Rad, Hercules, CA) [37, 38]. Equal amounts of RNA were reverse-transcribed using the iScript RT-PCR kit (Bio-Rad) according to manufacturer's instructions, and amplified in the presence of specific primers (all from IDT, Table 1) and iQ SYBR Green Supermix (Bio-Rad) at 60°C for 35 cycles. Transcript copy number was estimated by comparing to a serial dilution of cDNA for *Alpl*, encoding for alkaline phosphatase, and *Rpl38* (both from American Type Tissue Culture Collection, Manassas, VA), *Bglap*, encoding for osteocalcin (J. Lian, Burlington, VT), *Dll1* (E. Six, Paris, France), *Dll3*, *Dll4* and *Jag2* (GE Healthcare Dharmacon, Lafayette, CO), *Dmp1*, *Sost*, *Jag1* and *Notch2* (Thermo Fisher Scientific, Waltham, MA), *Hey1* and *Hey2* (T. Iso, Los Angeles, CA), *HeyL* (D. Srivastava, Dallas, TX), *Notch1* (J.S. Nye, Cambridge, MA), *Notch4* (Y. Shirayoshi, Tottori, Japan) and *Tnfsf11* (Source BioScience, Nottingham, UK) [39–44]. *Notch3* copy number was estimated by comparison to a serial dilution of a ~100 base pairs synthetic DNA template (IDT) cloned into pcDNA3.1(–) (Thermo Fisher Scientific) by isothermal single reaction assembly using commercially available reagents (New England BioLabs, Ipswich, MA) [45]. Reactions were conducted in a CFX96 qRT-PCR detection system (Bio-Rad), and fluorescence was

monitored during every PCR cycle at the annealing step. Data are expressed as copy number corrected for *Rpl38* [46].

2.4 Transient Transfections

A plasmid containing six dimeric consensus sequences for CSL, the human ortholog of Rbpjκ, upstream of the β-globin basal promoter and *Luciferase* (12xCSL-Luc; L.J. Strobl, Munich, Germany) was used to detect Rbpjκ-mediated transcriptional activity [47]. To induce Notch1, cells were co-transfected with a 2.4 kilobase DNA fragment containing the coding sequence of the murine Notch1 NICD (J.S. Nye) cloned into pcDNA3.1 downstream of the cytomegalovirus (CMV) promoter (pcDNA-NICD), or with control pcDNA3.1 [43]. Transfections were conducted in sub-confluent cultures of osteoblast-enriched cells with X-tremeGENE 9 (2 μl X-tremeGENE 9/1 μg DNA), according to manufacturer's instructions (Roche, Indianapolis, IN). A construct where the CMV promoter directs the expression of β-galactosidase (Clontech, Mountain View, CA) was used to correct for transfection efficiency. Cells were exposed to the X-tremeGENE 9/DNA mix for 16 h, transferred to DMEM without serum for 6 h, and exposed to PTH 10 nM or to vehicle for 24 h. Cells were harvested in reporter lysis buffer (Promega, Madison, WI) and lysed by freezing and thawing. Luciferase and β-galactosidase activity were determined with a luciferase assay system kit (Promega) and with galacton plus (Life Technologies), respectively, in accordance with manufacturers' instructions on an Optocomp II luminometer (MGM Instruments, Hamden, CT).

2.5 Electrophoretic Mobility Shift Assay (EMSA)

Nuclear extracts were obtained from wild-type osteoblast-enriched cells seeded on BSA or Dll1 and exposed either to vehicle or PTH at 10 nM. A double-stranded DNA oligonucleotide containing the *CSL* consensus sequence found in the Epstein-Barr virus nuclear antigen (EBNA)2 promoter (forward strand sequence: 5′-GGAAACACGCCGTGGGAAAAAATTTGGG-3′) biotinylated on both 5′-termini was synthesized commercially (IDT) [48]. Binding reactions of nuclear extracts with biotinylated DNA at a concentration of 1 μM were carried out with the LightShift Chemiluminescent EMSA Kit, as recommended by the manufacturer (Thermo Fisher Scientific). To determine the specificity of the interactions between the nuclear extracts and the biotinylated oligonucleotides, unlabeled homologous DNA was added in 200 fold excess. Nucleic acid-protein complexes were resolved on non-denaturing, non-reducing 4% polyacrylamide gels for 45 min and subsequently transferred to a nylon membrane with a 0.45 μm pore size (MP Biomedicals, Solon, OH) in 45 mM Tris, 45 mM boric acid, 1 mM EDTA at pH 8.3 (all from Sigma-Aldrich). Transfer was conducted for 30 min at 4°C, and crosslinking of the transferred complexes to the nylon membrane was carried out at 120 mJ/cm^2 for 1 min using a CL-1000 UV-light crosslinking instrument (UVP, Upland, CA). The biotinylated DNA was detected with a streptavidin-horseradish peroxidase conjugate following manufacturers' instructions for the LightShift Chemiluminescent EMSA Kit detection module, and images of chemiluminescence reactions were acquired with a Chemidoc XSR molecular imager (Bio-Rad).

2.6 Statistical Analysis

Data are expressed as means ± SEM. Statistical differences were determined by Student's *t* test or analysis of variance (ANOVA) with Holm-Šídák post-hoc analysis for pairwise or multiple comparisons, respectively.

3. RESULTS

3.1 PTH Suppresses Notch Signaling in Osteoblast-enriched Cells

To test the effects of PTH, osteoblast-enriched cells from the parietal bones of C57BL/6J wild-type mice were seeded on Dll1 for 24 h to activate Notch receptors or on BSA, and subsequently exposed to PTH or vehicle. Although Jag1 has a documented skeletal function, Dll1 was chosen because it enhances Notch activation consistently in multiple cell lineages and in osteoblasts, and both ligands induce Notch target genes to a comparable extent (Canalis and Zanotti unpublished observations) [49–51]. A PTH dose of 10 nM, known to have a maximal effect on osteoblast function was used for the present studies [52–55]. Cells cultured on Dll1 exhibited higher expression of the Notch target genes *Hey1*, *Hey2* and *HeyL* than those cultured on BSA, confirming activation of Notch signaling. Basal levels of *Hey1*, *Hey2* and *HeyL* mRNA obtained in the absence of Dll1 were not affected by PTH, but PTH opposed the effect of Dll1 on Notch activation reducing the expression of the three Notch target genes to basal levels (Figure 1).

3.2 Characterization of Osteocyte-enriched Cultures

To establish a cell culture system for the study of osteocytes *in vitro*, we obtained cells from sequential collagenase and EDTA digestions of femurs devoid of cartilage and bone marrow, and collected the resulting bone fragments after their final digestion with EDTA [34]. To identify the cell population with the highest enrichment in osteocytes, levels of transcripts for gene markers preferentially expressed by osteoblasts and osteocytes were determined. Expression of the osteoblastic markers *Alpl* and *Bglap* was detected in all cellular fractions and the digested femoral fragments displayed the highest levels of *Bglap* transcripts. Expression of *Dmp1* and *Sost* is higher in osteocytes than in osteoblasts, and both genes were detected only in bone fragments after their digestion with collagenase and EDTA, and these were considered osteocyte-enriched fractions (Figure 2) [4–6].

To determine the identity of the Notch paralogs and specific ligands expressed in the cellular fractions, mRNA levels for all Notch receptors, Jag and Dll ligands were measured. *Notch1* to *Notch4* had comparable expression levels and were detected in all fractions. Expression of *Notch1* and *Notch2* was more pronounced in fraction 5, whereas *Notch3* expression was highest in the osteocyte-enriched fraction. Expression of *Jag1* was uniform across all fractions while transcripts for *Dll1*, *Dll3*, *Dll4* and *Jag2* were not detected (Figure 2). Subsequently, femoral fragments were subjected to a single collagenase and an EDTA digestion and their treatment with PTH induced *Tnfsf11* and decreased *Sost* transcripts, confirming the known effects of PTH in osteocytes and documenting that the culture system is enriched in osteocytes (Figure 3) [11, 56].

3.3 PTH Inhibits Notch Signaling in Osteocyte-enriched Cultures

PTH suppressed the basal expression of the Notch target genes *Hey1*, *Hey2* and *HeyL* in osteocyte-enriched cultures, suggesting that mature osteoblastic cells are sensitized to the inhibitory effects of PTH on Notch signaling (Figure 4).

To determine the effects of PTH in the context of Notch activation in osteocytes, we tested the consequences of PTH exposure in osteocyte-enriched cells from heterozygous *Notch2HCS* mice, a model of *Notch2* gain-of-function [25]. This was necessary because bone fragments cannot be acutely transfected with Notch expression vectors nor successfully cultured on Notch-specific ligands to achieve activation. In the absence of PTH, osteocyte-enriched cells from *Notch2HCS* mice exhibited higher *Hey1*, *Hey2* and *HeyL* mRNA levels than those from wild-type littermates, confirming activation of Notch signaling (Figure 5). PTH opposed basal and Notch2-induced expression of *Hey1* and *Hey2* transcripts. PTH suppressed *HeyL* in cultures from wild-type mice by ~50%, although the effect did not reach statistical significance, and PTH did not alter *HeyL* mRNA levels in bone fragments from *Notch2HCS* mutants (Figure 5). The reason for the sustained expression of *HeyL* in the presence of PTH remains without an obvious explanation. Confirming previous results, PTH induced *Tnfsf11* and suppressed *Sost* expression in cultures from *Notch2HCS* mutants and wild-type littermates. *Notch2* had a lesser effect than PTH on *Tnfsf11* and *Sost* expression, and no additive or synergetic effects with PTH were observed.

3.4 PTH Suppresses Notch Signaling In Vivo

To establish whether PTH regulates Notch signaling in osteoblastic cells *in vivo*, 1 month old C57BL/6J wild-type male mice were administered with PTH 80 μg/Kg or vehicle, and the expression of Notch target genes was measured in parietal bones 3 h after injection. PTH suppressed *Hey1* and *HeyL* mRNA levels, but not *Hey2* (Figure 6). Confirming previous observations, PTH downregulated *Sost* mRNA levels [11].

3.5 PTH Inhibits Rbpjκ-mediated Notch Signaling

To determine whether the inhibition of Notch target gene expression by PTH is mediated by an effect on Rbpjκ-mediated signaling, wild-type osteoblasts were transiently transfected with the 12xCSL-Luc reporter, which contains consensus sequences for CSL, the human ortholog for Rbpjk. Cells were co-transfected with pcDNA-NICD to overexpress Notch, or a control vector, and exposed to either PTH or vehicle. Transactivation of the 12xCSL-Luc construct was detected only in cells co-transfected with pcDNA-NICD and PTH reduced luciferase activity by ~70%, indicating that PTH inhibits Rbpjκ-mediated Notch signaling (Figure 7A).

To explore the mechanisms responsible for the inhibition of Notch signaling by PTH, EMSA were carried out in osteoblast-enriched cells harvested from C57BL/6J wild-type mice and seeded on Dll1, to induce Notch, or on BSA. A biotinylated oligonucleotide containing the consensus sequence for *CSL* was bound by nuclear protein extracts from cells cultured on BSA, and an excess of unlabeled *CSL* oligonucleotides prevented this effect, demonstrating specificity of the protein-DNA interaction. In cells cultured on BSA, PTH suppressed the formation of nuclear protein complexes with the biotinylated *CSL* consensus

oligonucleotide, supporting the notion that PTH prevents the interaction of Rbpjκ with DNA (Figure 7B). Previous reports demonstrated that the binding of Rbpjκ to DNA oligonucleotides decreases in the presence of active Notch receptors; similarly, a nuclear protein-*CSL* consensus oligonucleotide complex was not observed in osteoblasts seeded on Dll1 [57]. The complex was partially restored in cultures exposed to both Dll1 and PTH, suggesting that activation of the Notch receptors interferes with the inhibitory effects of PTH on the ability of Rbpjκ to bind DNA (Figure 7B).

4. DISCUSSION

The present work demonstrates that PTH suppresses Notch signaling in osteoblasts and osteocytes. Expression of the four Notch receptors was documented in both cell types, suggesting that PTH affects a signaling mechanism that may be common to all Notch paralogs. Inhibition of Notch target gene expression was observed at a concentration of PTH that regulates parameters of osteoblastic function, such as *Alpl*, *Col1a1*, *Igf1* and *Bglap* expression and collagen type I synthesis, [52–55] (Zanotti and Canalis unpublished). Suppression of Notch signaling is an acute response to PTH that includes inhibition of Rbpjκ/DNA interactions and of Notch transactivating capacity. In contrast, the regulation of osteoblastic function is noted after longer exposure to PTH, suggesting that PTH regulates activation of Notch directly [52–55]. Notch activation during the early stages of the osteoblast differentiation program suppresses bone formation and leads to osteopenia, whereas PTH enhances bone formation in rodents and humans [12, 21–24]. Therefore, suppression of Notch signaling by PTH may be required to achieve an optimal anabolic response to the hormone.

The current work confirmed the effects of PTH on *Tnfsf11* expression in osteoblast-enriched cells and those of PTH and Notch on *Tnfsf11* and *Sost* transcripts in cultures of osteocyte-enriched femoral fragments. These results indicate that the osteocyte-enriched cultures used in the present work are a viable model to investigate osteocyte biology. However, studies in this system must be interpreted with caution, since expression of *Alpl* indicates the possible presence of contaminating osteoblasts in femoral fragments. It is of interest that PTH induced *Tnfsf11* expression to a greater extent in osteocyte-enriched cultures (~30 fold) than in primary osteoblasts (~3 fold). This is in accordance with the fundamental role of osteocyte-derived Rankl in bone resorption [58, 59]. The suppression of *Sost* mRNA levels *in vivo* is consistent with the bone anabolic response to PTH [1]. The effects of Notch on *Tnfsf11* and *Sost* expression were less pronounced than those of PTH, and Notch activation did not enhance the effect of PTH on either gene.

Transactivation and EMSA experiments conducted in osteoblast-enriched cultures suggest that PTH opposes Notch signaling by decreasing the capacity of Rbpjκ to associate with DNA and also by interfering with the formation of an active NICD/Rbpjκ transcriptional complex. These effects are mediated by intracellular events, since Notch signaling was suppressed in the context of the Notch1 NICD overexpression, which is a model of activation that does not require the presence of ligands or cleavage of the extracellular domain of the receptor [43]. The partial restoration of the complex in the presence of PTH and Dll1 suggests that the nuclear translocation of the NICD may lessen the inhibitory effect

of PTH on the ability of Rbpjκ to bind to DNA. This mechanism may explain the residual expression of Notch target genes in the context of PTH exposure. In the present study, known limitations to the study of Rbpjk/DNA interactions by EMSA are documented. Namely, displaced *CSL* probes are not always visible in the presence of unlabeled competitors, and formation of an active transcriptional complex in the context of Dll1 exposure may lead to a shift of the nuclear protein bound to the CSL probe and attenuation of the signal [57, 60, 61]. Although the identity of the factors that prevent the association of Rbpjκ with DNA is not known, activation of MAPK in response to PTH may be involved in this process. Previous work demonstrated that selected members of the MAPK family are expressed by osteoblasts, regulate bone remodeling, and can prevent the formation of an active Notch transcriptional complex [62–65]. Another alternative is activation of cyclic AMP, a mechanism that has been found to be responsible for the downregulation of Sost in osteocytes expressing a constitutively active form of the PTH receptor [66, 67].

The inhibitory effect of PTH on Notch signaling is analogous to the one reported for nuclear factor of activated T-cells (Nfatc)1 and Nfatc2 [22, 68]. In the present studies, we tested and determined that PTH induces Nfatc1 and Nfatc2 in osteocyte-enriched cultures, but not in calvarial osteoblasts (Zanotti and Canalis unpublished). However, since suppression of Notch signaling was observed in both cell preparations, it is probably not related to an induction of Nfatc1 or Nfatc2. Although the effect of PTH in osteocytes was assessed by examining for the downregulation of Notch target genes and not by transactivation or EMSA experiments, it is probable that PTH acts by similar mechanisms in both osteoblasts and osteocytes [19]. Additional osteocyte-specific mechanisms may be operational, since in contrast to the observations in osteoblast cultures, PTH suppressed *Hey* expression in osteocytes even in the absence of Notch activation. This suggests a sensitization to the effects of PTH on Notch signaling or higher basal levels of *Hey1*, *Hey2* and *HeyL* transcripts in osteocytes than in osteoblasts. Moreover, the expression of Notch3 in osteocyte-enriched cells may be accountable for the different response of osteocytes and osteoblasts to PTH, since the Notch3 receptor exhibits higher degree of basal activation than Notch1 and Notch2 [69].

The effect of PTH was observed in osteocyte cultures from *Notch2HCS* mice expressing a truncated and stable Notch2 NICD that is resistant to proteasomal degradation [70]. This would suggest that PTH is not likely to act by destabilizing the Notch NICD. The relative increase in *Hey1* and *Hey2* mRNA levels in the context of the *Notch2HCS* mutation was not affected by PTH. This indicates that suppression of *Hey1* and *Hey2* expression occurs by mechanisms that do not require inhibition of Notch2 or Rbpjκ function and may be secondary to an effect of PTH on the osteocytic phenotype. PTH did not suppress *HeyL* expression in the context of the *Notch2HCS* mutation. The reason is not known, but recent work has shown that the NICD of Notch1 and Notch2 activate transcription by associating with distinct regions of Rbpjκ, and that the structure of the target gene promoter determines differences in the capacity of Notch to induce transcription [71]. It is possible that the association of the Notch2 NICD with Rbpjκ bound to *HeyL* regulatory sequences was not affected by the mechanisms that mediate the inhibitory effects of PTH on *Hey1* and *Hey2*.

Previous work demonstrated that PTH induces the Notch ligand Jag1 in cells of the osteoblastic lineage and in the bone marrow niche with an apparent increase in Notch signaling [28, 29]. Although we confirmed this effect (Zanotti and Canalis unpublished) and reported that Jag1 is the only Notch specific ligand expressed by osteoblastic cells in femurs, we observed that PTH downregulates Notch signaling in osteoblasts and osteocytes. A possible explanation is that *Jag1* induction is not sufficient to overcome the inhibitory effect of PTH on Rbpjκ-mediated signaling that occurs primarily in the osteoblastic lineage but might not take place in the bone marrow niche. Alternatively, Jag1 induced by PTH may sequester and suppress Notch receptors with a mechanism of *cis*-inhibition that takes place when receptors and ligands are expressed by the same cell and is known to occur in *Drosophila* and mammalian cells [72].

In conclusion, PTH prevents the association of Rbpjκ with DNA and suppresses Notch signaling in the osteoblastic lineage, effects that may contribute to the anabolic actions of PTH in bone.

Acknowledgments

The authors thank J. Lian for Bglap cDNA, E. Six for Dll1 cDNA, T. Iso for Hey1 and Hey2 cDNAs, D. Srivastava for HeyL cDNA, Y. Shirayoshi for Notch4 cDNA, L.J. Strobl for 12xCSL-Luc and J.S. Nye for the pcDNA-NICD. The authors thank D. Bridgewater, T. Eller, and L. Schilling for technical assistance and M. Yurczak for secretarial support.

*This work was supported by [Grants AR063049 and AR068160] from the National Institute of Arthritis and Musculoskeletal and Skin Diseases (NIAMS) and [Grant DK045227] from the National Institute of Diabetes and Digestive and Kidney Diseases (NIDDK). The content is solely the responsibility of the authors and does not necessarily represent the official views of the National Institutes of Health.

ABBREVIATIONS

ANOVA	analysis of variance
BSA	bovine serum albumin
CMV	cytomegalovirus
CSL	core binding factor-1/suppressor of hairless/Lag-1
Dll	delta-like
DMEM	Dulbecco’s modified Eagle’s medium
Dmp	dentin matrix protein
EBNA	Epstein-Barr virus nuclear antigen
EMSA	electrophoretic mobility shift assay
FBS	fetal bovine serum
GFP	green fluorescent protein
HCS	Hajdu Cheney syndrome

IDT	Integrated DNA Technologies
Jag	Jagged
MAPK	mitogen activated protein kinase
Nfatc	nuclear factor of activated T-cells
NICD	Notch intracellular domain
PBS	phosphate buffered saline
PCR	polymerase chain reaction
PEST	proline-, glutamic acid-, serine- and threonine-rich
PTH	parathyroid hormone 1–34 fragment
qRT-PCR	quantitative reverse transcription-PCR
Rankl	Receptor activator of nuclear factor kappa B ligand
Rbpjκ	recombination signal binding protein J kappa
SEM	standard error of the mean
TLCK	N-α-tosyl-L-lysyl-chloromethylketone hydrochloride

References

1. Canalis E, Giustina A, Bilezikian JP. Mechanisms of anabolic therapies for osteoporosis. The New England journal of medicine. 2007; 357(9):905–16. DOI: 10.1056/NEJMra067395 [PubMed: 17761594]
2. Dallas SL, Prideaux M, Bonewald LF. The osteocyte: an endocrine cell … and more, Endocr. Rev. 2013; 34(5):658–90. DOI: 10.1210/er.2012-1026
3. Lacey DL, Timms E, Tan HL, Kelley MJ, Dunstan CR, Burgess T, Elliott R, Colombero A, Elliott G, Scully S, Hsu H, Sullivan J, Hawkins N, Davy E, Capparelli C, Eli A, Qian YX, Kaufman S, Sarosi I, Shalhoub V, Senaldi G, Guo J, Delaney J, Boyle WJ. Osteoprotegerin ligand is a cytokine that regulates osteoclast differentiation and activation. Cell. 1998; 93(2):165–176. [PubMed: 9568710]
4. Brunkow ME, Gardner JC, Van Ness J, Paeper BW, Kovacevich BR, Proll S, Skonier JE, Zhao L, Sabo PJ, Fu Y, Alisch RS, Gillett L, Colbert T, Tacconi P, Galas D, Hamersma H, Beighton P, Mulligan J. Bone dysplasia sclerosteosis results from loss of the SOST gene product, a novel cystine knot-containing protein. Am J Hum Genet. 2001; 68(3):577–89. [PubMed: 11179006]
5. Nioi P, Taylor S, Hu R, Pacheco E, He YD, Hamadeh H, Paszty C, Pyrah I, Ominsky MS, Boyce RW. Transcriptional Profiling of Laser Capture Microdissected Subpopulations of the Osteoblast Lineage Provides Insight Into the Early Response to Sclerostin Antibody in Rats. J Bone Miner Res. 2015; 30(8):1457–67. DOI: 10.1002/jbmr.2482 [PubMed: 25678055]
6. Xiong J, Piemontese M, Onal M, Campbell J, Goellner JJ, Dusevich V, Bonewald L, Manolagas SC, O'Brien CA. Osteocytes, not Osteoblasts or Lining Cells, are the Main Source of the RANKL Required for Osteoclast Formation in Remodeling Bone. PLoS One. 2015; 10(9):e0138189.doi: 10.1371/journal.pone.0138189 [PubMed: 26393791]
7. Bezooijen, RLvan, Roelen, BA., Visser, A., Wee-Pals, Lvander, Wilt, Ede, Karperien, M., Hamersma, H., Papapoulos, SE., Dijke, Pten, Lowik, CW. Sclerostin is an osteocyte-expressed negative regulator of bone formation, but not a classical BMP antagonist. J Exp Med. 2004; 199(6): 805–14. DOI: 10.1084/jem.20031454 [PubMed: 15024046]

8. Murray TM, Rao LG, Divieti P, Bringhurst FR. Parathyroid hormone secretion and action: evidence for discrete receptors for the carboxyl-terminal region and related biological actions of carboxyl-terminal ligands. Endocrine reviews. 2005; 26(1):78–113. DOI: 10.1210/er.2003-0024 [PubMed: 15689574]
9. Rouleau MF, Mitchell J, Goltzman D. In vivo distribution of parathyroid hormone receptors in bone: evidence that a predominant osseous target cell is not the mature osteoblast. Endocrinology. 1988; 123(1):187–91. DOI: 10.1210/endo-123-1-187 [PubMed: 2838253]
10. Fermor B, Skerry TM. PTH/PTHrP receptor expression on osteoblasts and osteocytes but not resorbing bone surfaces in growing rats. J Bone Miner Res. 1995; 10(12):1935–43. DOI: 10.1002/jbmr.5650101213 [PubMed: 8619374]
11. Bellido T, Ali AA, Gubrij I, Plotkin LI, Fu Q, O'Brien CA, Manolagas SC, Jilka RL. Chronic elevation of parathyroid hormone in mice reduces expression of sclerostin by osteocytes: a novel mechanism for hormonal control of osteoblastogenesis. Endocrinology. 2005; 146(11):4577–83. DOI: 10.1210/en.2005-0239 [PubMed: 16081646]
12. Canalis E. Update in new anabolic therapies for osteoporosis. J Clin Endocrinol Metab. 2010; 95(4):1496–504. DOI: 10.1210/jc.2009-2677 [PubMed: 20375217]
13. Kedlaya R, Kang KS, Hong JM, Bettagere V, Lim KE, Horan D, Divieti-Pajevic P, Robling AG. Adult-Onset Deletion of beta-Catenin in (10kb)Dmp1-Expressing Cells Prevents Intermittent PTH-Induced Bone Gain. Endocrinology. 2016; 157(8):3047–57. DOI: 10.1210/en.2015-1587 [PubMed: 27253995]
14. Robling AG, Kedlaya R, Ellis SN, Childress PJ, Bidwell JP, Bellido T, Turner CH. Anabolic and catabolic regimens of human parathyroid hormone 1–34 elicit bone- and envelope-specific attenuation of skeletal effects in Sost-deficient mice. Endocrinology. 2011; 152(8):2963–75. DOI: 10.1210/en.2011-0049 [PubMed: 21652726]
15. Fu Q, Jilka RL, Manolagas SC, O'Brien CA. Parathyroid hormone stimulates receptor activator of NFkappa B ligand and inhibits osteoprotegerin expression via protein kinase A activation of cAMP-response element-binding protein. J Biol Chem. 2002; 277(50):48868–75. DOI: 10.1074/jbc.M208494200 [PubMed: 12364326]
16. Yasuda H, Shima N, Nakagawa N, Yamaguchi K, Kinosaki M, Mochizuki S, Tomoyasu A, Yano K, Goto M, Murakami A, Tsuda E, Morinaga T, Higashio K, Udagawa N, Takahashi N, Suda T. Osteoclast differentiation factor is a ligand for osteoprotegerin/osteoclastogenesis-inhibitory factor and is identical to TRANCE/RANKL, Proc. Natl Acad Sci U S A. 1998; 95(7):3597–602.
17. Mahalingam CD, Sampathi BR, Sharma S, Datta T, Das V, Abou-Samra AB, Datta NS. MKP1-dependent PTH modulation of bone matrix mineralization in female mice is osteoblast maturation stage specific and involves P-ERK and P-p38 MAPKs. J Endocrinol. 2013; 216(3):315–29. DOI: 10.1530/joe-12-0372 [PubMed: 23197743]
18. Kopan R, Ilagan MX. The canonical Notch signaling pathway: unfolding the activation mechanism. Cell. 2009; 137(2):216–33. DOI: 10.1016/j.cell.2009.03.045 [PubMed: 19379690]
19. Iso T, Kedes L, Hamamori Y. HES and HERP families: multiple effectors of the Notch signaling pathway. J Cell Physiol. 2003; 194(3):237–55. DOI: 10.1002/jcp.10208 [PubMed: 12548545]
20. Zanotti S, Canalis E. Notch Signaling and the Skeleton. Endocr Rev. 2016; 37(3):223–53. DOI: 10.1210/er.2016-1002 [PubMed: 27074349]
21. Zanotti S, Smerdel-Ramoya A, Stadmeyer L, Durant D, Radtke F, Canalis E. Notch inhibits osteoblast differentiation and causes osteopenia. Endocrinology. 2008; 149(8):3890–9. DOI: 10.1210/en.2008-0140 [PubMed: 18420737]
22. Zanotti S, Smerdel-Ramoya A, Canalis E. Reciprocal regulation of Notch and nuclear factor of activated T-cells (NFAT) c1 transactivation in osteoblasts. J Biol Chem. 2011; 286(6):4576–88. DOI: 10.1074/jbc.M110.161893 [PubMed: 21131365]
23. Canalis E, Adams DJ, Boskey A, Parker K, Kranz L, Zanotti S. Notch Signaling in Osteocytes Differentially Regulates Cancellous and Cortical Bone Remodeling. J Biol Chem. 2013; 288(35):25614–25625. M113.470492 [pii];10.1074/jbc.M113.470492 [doi]. [PubMed: 23884415]
24. Canalis E, Parker K, Feng JQ, Zanotti S. Osteoblast Lineage-specific Effects of Notch Activation in the Skeleton. Endocrinology. 2013; 154(2):623–634. en.2012-1732 [pii];10.1210/en.2012-1732 [doi]. [PubMed: 23275471]

25. Canalis E, Schilling L, Yee SP, Lee SK, Zanotti S. Hajdu Cheney Mouse Mutants Exhibit Osteopenia, Increased Osteoclastogenesis and Bone Resorption. J Biol Chem. 2016; 291:1538–1551. DOI: 10.1074/jbc.M115.685453 [PubMed: 26627824]
26. Yorgan T, Vollersen N, Riedel C, Jeschke A, Peters S, Busse B, Amling M, Schinke T. Osteoblast-specific Notch2 inactivation causes increased trabecular bone mass at specific sites of the appendicular skeleton. Bone. 2016; 87:136–146. DOI: 10.1016/j.bone.2016.04.012 [PubMed: 27102824]
27. Canalis E, Bridgewater D, Schilling L, Zanotti S. Canonical Notch Activation in Osteocytes Causes Osteopetrosis, American journal of physiology. Endocrinology and metabolism. 2015; 310(2):E171–E182. DOI: 10.1152/ajpendo.00395.2015 [PubMed: 26578715]
28. Weber JM, Forsythe SR, Christianson CA, Frisch BJ, Gigliotti BJ, Jordan CT, Milner LA, Guzman ML, Calvi LM. Parathyroid hormone stimulates expression of the Notch ligand Jagged1 in osteoblastic cells. Bone. 2006; 39(3):485–93. DOI: 10.1016/j.bone.2006.03.002 [PubMed: 16647886]
29. Calvi LM, Adams GB, Weibrecht KW, Weber JM, Olson DP, Knight MC, Martin RP, Schipani E, Divieti P, Bringhurst FR, Milner LA, Kronenberg HM, Scadden DT. Osteoblastic cells regulate the haematopoietic stem cell niche. Nature. 2003; 425(6960):841–6. DOI: 10.1038/nature02040 [PubMed: 14574413]
30. Duggan SP, McCarthy JV. Beyond gamma-secretase activity: The multifunctional nature of presenilins in cell signalling pathways. Cell Signal. 2016; 28(1):1–11. DOI: 10.1016/j.cellsig.2015.10.006
31. Zanotti S, Kalajzic I, Aguila HL, Canalis E. Sex and genetic factors determine osteoblastic differentiation potential of murine bone marrow stromal cells. PLoS One. 2014; 9(1):e86757. [doi];PONE-D-13-31354 [pii]. doi: 10.1371/journal.pone.0086757 [PubMed: 24489784]
32. Hsu H, Lacey DL, Dunstan CR, Solovyev I, Colombero A, Timms E, Tan HL, Elliott G, Kelley MJ, Sarosi I, Wang L, Xia XZ, Elliott R, Chiu L, Black T, Scully S, Capparelli C, Morony S, Shimamoto G, Bass MB, Boyle WJ. Tumor necrosis factor receptor family member RANK mediates osteoclast differentiation and activation induced by osteoprotegerin ligand. Proc Natl Acad Sci U S A. 1999; 96(7):3540–5. [PubMed: 10097072]
33. Centrella M, McCarthy TL, Canalis E. Parathyroid hormone modulates transforming growth factor beta activity and binding in osteoblast-enriched cell cultures from fetal rat parietal bone. Proc Natl Acad Sci U S A. 1988; 85(16):5889–93. [PubMed: 2901093]
34. Halleux C, Kramer I, Allard C, Kneissel M. Isolation of mouse osteocytes using cell fractionation for gene expression analysis. Methods Mol Biol. 2012; 816:55–66. [doi]. DOI: 10.1007/978-1-61779-415-5_5 [PubMed: 22130922]
35. Zanotti S, Canalis E. The Dmp1-SOST Transgene Interacts With and Downregulates the Dmp1-Cre Transgene and the Rosa Allele. J Cell Biochem. 2015; doi: 10.1002/jcb.25405
36. Canalis E, Zanotti S. Hairy and Enhancer of Split-related with YRPW Motif-Like (HeyL) is Dispensable for Bone Remodeling in Mice. J Cell Biochem. 2016; doi: 10.1002/jcb.25859
37. Nazarenko I, Lowe B, Darfler M, Ikonomi P, Schuster D, Rashtchian A. Multiplex quantitative PCR using self-quenched primers labeled with a single fluorophore. Nucleic Acids Res. 2002; 30(9):e37. [PubMed: 11972352]
38. Nazarenko I, Pires R, Lowe B, Obaidy M, Rashtchian A. Effect of primary and secondary structure of oligodeoxyribonucleotides on the fluorescent properties of conjugated dyes. Nucleic Acids Res. 2002; 30(9):2089–195. [PubMed: 11972350]
39. Lian J, Stewart C, Puchacz E, Mackowiak S, Shalhoub V, Collart D, Zambetti G, Stein G. Structure of the rat osteocalcin gene and regulation of vitamin D-dependent expression. Proc Natl Acad Sci USA. 1989; 86(4):1143–7. [PubMed: 2784002]
40. Six EM, Ndiaye D, Sauer G, Laabi Y, Athman R, Cumano A, Brou C, Israel A, Logeat F. The notch ligand Delta1 recruits Dlg1 at cell-cell contacts and regulates cell migration. J Biol Chem. 2004; 279(53):55818–26. DOI: 10.1074/jbc.M408022200 [PubMed: 15485825]
41. Iso T, Sartorelli V, Chung G, Shichinohe T, Kedes L, Hamamori Y. HERP, a new primary target of Notch regulated by ligand binding. Mol Cell Biol. 2001; 21(17):6071–9. [PubMed: 11486044]

42. Nakagawa O, Nakagawa M, Richardson JA, Olson EN, Srivastava D. HRT1, HRT2, and HRT3: a new subclass of bHLH transcription factors marking specific cardiac, somitic, and pharyngeal arch segments. Dev Biol. 1999; 216(1):72–84. [doi];S0012-1606(99)99454-X [pii]. DOI: 10.1006/dbio.1999.9454 [PubMed: 10588864]
43. Nye JS, Kopan R, Axel R. An activated Notch suppresses neurogenesis and myogenesis but not gliogenesis in mammalian cells. Development. 1994; 120(9):2421–2430. [PubMed: 7956822]
44. Shirayoshi Y, Yuasa Y, Suzuki T, Sugaya K, Kawase E, Ikemura T, Nakatsuji N. Proto-oncogene of int-3, a mouse Notch homologue, is expressed in endothelial cells during early embryogenesis. Genes Cells. 1997; 2(3):213–224. [PubMed: 9189758]
45. Gibson DG, Young L, Chuang RY, Venter JC, Hutchison CA 3rd, Smith HO. Enzymatic assembly of DNA molecules up to several hundred kilobases. Nat Methods. 2009; 6(5):343–5. DOI: 10.1038/nmeth.1318 [PubMed: 19363495]
46. Kouadjo KE, Nishida Y, Cadrin-Girard JF, Yoshioka M, St-Amand J. Housekeeping and tissue-specific genes in mouse tissues. BMC Genomics. 2007; 8:127.doi: 10.1186/1471-2164-8-127 [PubMed: 17519037]
47. Strobl LJ, Hofelmayr H, Stein C, Marschall G, Brielmeier M, Laux G, Bornkamm GW, Zimber-Strobl U. Both Epstein-Barr viral nuclear antigen 2 (EBNA2) and activated Notch1 transactivate genes by interacting with the cellular protein RBP-J kappa. Immunobiology. 1997; 198(1–3):299–306. [PubMed: 9442401]
48. Henkel T, Ling PD, Hayward SD, Peterson MG. Mediation of Epstein-Barr virus EBNA2 transactivation by recombination signal-binding protein J kappa. Science (New York, NY). 1994; 265(5168):92–5.
49. Canalis E, Zanotti S, Smerdel-Ramoya A. Connective Tissue Growth Factor is a Target of Notch Signaling in Cells of the Osteoblastic Lineage. Bone. 2014; 64:273–280. S8756–3282(14)00163-X [pii];10.1016/j.bone.2014.04.028 [doi]. [PubMed: 24792956]
50. Youngstrom DW, Dishowitz MI, Bales CB, Carr E, Mutyaba PL, Kozloff KM, Shitaye H, Hankenson KD, Loomes KM. Jagged1 expression by osteoblast-lineage cells regulates trabecular bone mass and periosteal expansion in mice. Bone. 2016; 91:64–74. DOI: 10.1016/j.bone.2016.07.006 [PubMed: 27416809]
51. Lawal RA, Zhou X, Batey K, Hoffman CM, Georger MA, Radtke F, Hilton MJ, Xing L, Frisch BJ, Calvi LM. The Notch Ligand Jagged1 Regulates the Osteoblastic Lineage by Maintaining the Osteoprogenitor Pool. J Bone Miner Res. 2017; doi: 10.1002/jbmr.3106
52. Dietrich JW, Canalis EM, Maina DM, Raisz LG. Hormonal control of bone collagen synthesis in vitro: effects of parathyroid hormone and calcitonin. Endocrinology. 1976; 98(4):943–949. [PubMed: 945152]
53. Canalis E. Effect of hormones and growth factors on alkaline phosphatase activity and collagen synthesis in cultured rat calvariae. Metabolism. 1983; 32(1):14–20. [PubMed: 6217395]
54. Noda M, Yoon K, Rodan GA. Cyclic AMP-mediated stabilization of osteocalcin mRNA in rat osteoblast-like cells treated with parathyroid hormone. J Biol Chem. 1988; 263(34):18574–7. [PubMed: 2461371]
55. McCarthy TL, Centrella M, Canalis E. Parathyroid hormone enhances the transcript and polypeptide levels of insulin-like growth factor I in osteoblast-enriched cultures from fetal rat bone. Endocrinology. 1989; 124(3):1247–1253. [PubMed: 2645113]
56. Lee SK, Lorenzo JA. Parathyroid hormone stimulates TRANCE and inhibits osteoprotegerin messenger ribonucleic acid expression in murine bone marrow cultures: correlation with osteoclast-like cell formation. Endocrinology. 1999; 140(8):3552–61. DOI: 10.1210/endo.140.8.6887 [PubMed: 10433211]
57. Oswald F, Tauber B, Dobner T, Bourteele S, Kostezka U, Adler G, Liptay S, Schmid RM. p300 acts as a transcriptional coactivator for mammalian Notch-1, Mol. Cell Biol. 2001; 21(22):7761–7774.
58. Nakashima T, Hayashi M, Fukunaga T, Kurata K, Oh-Hora M, Feng JQ, Bonewald LF, Kodama T, Wutz A, Wagner EF, Penninger JM, Takayanagi H. Evidence for osteocyte regulation of bone homeostasis through RANKL expression. Nat Med. 2011; 17(10):1231–1234. nm.2452 [pii]; 10.1038/nm.2452 [doi]. [PubMed: 21909105]

59. Xiong J, Onal M, Jilka RL, Weinstein RS, Manolagas SC, O'Brien CA. Matrix-embedded cells control osteoclast formation. Nat Med. 2011; 17(10):1235–1241. nm.2448 [pii];10.1038/nm.2448 [doi]. [PubMed: 21909103]
60. Liang Y, Ganem D. RBP-J (CSL) is essential for activation of the K14/vGPCR promoter of Kaposi's sarcoma-associated herpesvirus by the lytic switch protein RTA. J Virol. 2004; 78(13): 6818–26. DOI: 10.1128/jvi.78.13.6818-6826.2004 [PubMed: 15194757]
61. Shi M, Hu ZL, Zheng MH, Song NN, Huang Y, Zhao G, Han H, Ding YQ. Notch-Rbpj signaling is required for the development of noradrenergic neurons in the mouse locus coeruleus. J Cell Sci. 2012; 125(Pt 18):4320–32. DOI: 10.1242/jcs.102152 [PubMed: 22718343]
62. Canalis E, Kranz L, Zanotti S. Nemo-like kinase regulates postnatal skeletal homeostasis. J Cell Physiol. 2014; 229(11):1736–43. DOI: 10.1002/jcp.24625 [PubMed: 24664870]
63. Ishitani T, Hirao T, Suzuki M, Isoda M, Ishitani S, Harigaya K, Kitagawa M, Matsumoto K, Itoh M. Nemo-like kinase suppresses Notch signalling by interfering with formation of the Notch active transcriptional complex. Nat Cell Biol. 2010; 12(3):278–85. DOI: 10.1038/ncb2028 [PubMed: 20118921]
64. Zanotti S, Canalis E. Nemo-like kinase inhibits osteoblastogenesis by suppressing bone morphogenetic protein and WNT canonical signaling. J Cell Biochem. 2012; 113(2):449–456. [doi]. DOI: 10.1002/jcb.23365 [PubMed: 21928348]
65. Nifuji A, Ideno H, Ohyama Y, Takanabe R, Araki R, Abe M, Noda M, Shibuya H. Nemo-like kinase (NLK) expression in osteoblastic cells and suppression of osteoblastic differentiation. Exp Cell Res. 2010; 316(7):1127–36. DOI: 10.1016/j.yexcr.2010.01.023 [PubMed: 20116374]
66. O'Brien CA, Plotkin LI, Galli C, Goellner JJ, Gortazar AR, Allen MR, Robling AG, Bouxsein M, Schipani E, Turner CH, Jilka RL, Weinstein RS, Manolagas SC, Bellido T. Control of bone mass and remodeling by PTH receptor signaling in osteocytes. PLoS One. 2008; 3(8):e2942.doi: 10.1371/journal.pone.0002942 [PubMed: 18698360]
67. Schipani E, Kruse K, Juppner H. A constitutively active mutant PTH-PTHrP receptor in Jansen-type metaphyseal chondrodysplasia. Science (New York, NY). 1995; 268(5207):98–100.
68. Zanotti S, Smerdel-Ramoya A, Canalis E. Nuclear Factor of Activated T-cells (Nfat)c2 Inhibits Notch Signaling in Osteoblasts. J Biol Chem. 2013; 288(1):624–632. M112.340455 [pii];10.1074/jbc.M112.340455 [doi]. [PubMed: 23166323]
69. Xu X, Choi SH, Hu T, Tiyanont K, Habets R, Groot AJ, Vooijs M, Aster JC, Chopra R, Fryer C, Blacklow SC. Insights into Autoregulation of Notch3 from Structural and Functional Studies of Its Negative Regulatory Region. Structure. 2015; 23(7):1227–35. DOI: 10.1016/j.str.2015.05.001 [PubMed: 26051713]
70. Oberg C, Li J, Pauley A, Wolf E, Gurney M, Lendahl U. The Notch intracellular domain is ubiquitinated and negatively regulated by the mammalian Sel-10 homolog. J Biol Chem. 2001; 276(38):35847–53. DOI: 10.1074/jbc.M103992200 [PubMed: 11461910]
71. Yuan Z, Friedmann DR, Vanderwielen BD, Collins KJ, Kovall RA. Characterization of CSL (CBF-1, Su(H), Lag-1) Mutants Reveals Differences in Signaling Mediated by Notch1 and Notch2. J Biol Chem. 2012; 287(42):34904–34916. M112.403287 [pii];10.1074/jbc.M112.403287 [doi]. [PubMed: 22915591]
72. del Alamo D, Rouault H, Schweisguth F. Mechanism and significance of cis-inhibition in Notch signalling. Curr Biol. 2011; 21(1):R40–7. DOI: 10.1016/j.cub.2010.10.034 [PubMed: 21215938]

HIGHLIGHTS

- PTH and Notch regulate bone formation
- PTH suppresses Notch signaling in osteoblasts and osteocytes *in vitro*
- PTH suppresses Notch signaling in bone *in vivo*
- Suppression of Notch may contribute to the bone anabolic effects of PTH

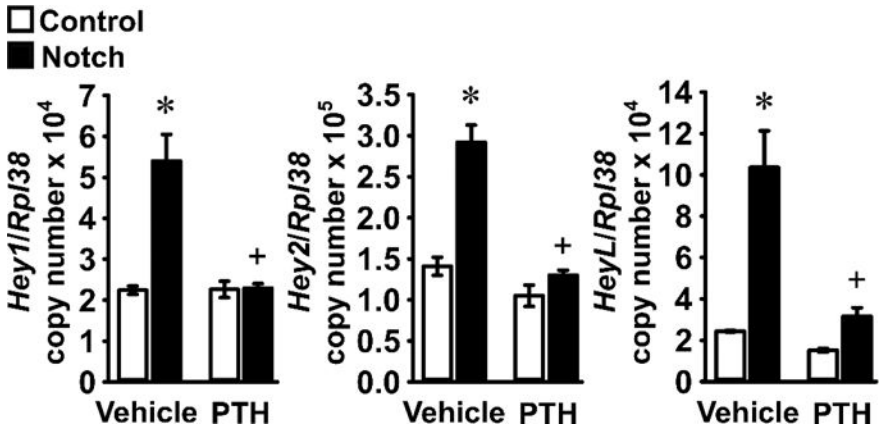

Figure 1. PTH prevents the induction of Notch target genes in osteoblasts

Primary osteoblast-enriched cells were harvested from parietal bones of 3 to 5 day old wild-type C57BL/6J mice and seeded on BSA (Control, white bars) or Dll1 (Notch, black bars) coated culture plates. After confluence, cells were cultured for 24 h in the absence of serum and exposed to vehicle or PTH at 10 nM (PTH) for 6 h. Total RNA was extracted and mRNA levels quantified by qRT-PCR in the presence of specific primers. Data are expressed as *Hey1*, *Hey2* and *HeyL* copy number corrected for *Rpl38* expression. Values are means ± SEM; n = 3 – 4. *Significantly different between Control and Notch, $p < 0.05$; $^{+}$significantly different between Vehicle and PTH, $p < 0.05$; two-way ANOVA with Holm-Šídák post-hoc analysis.

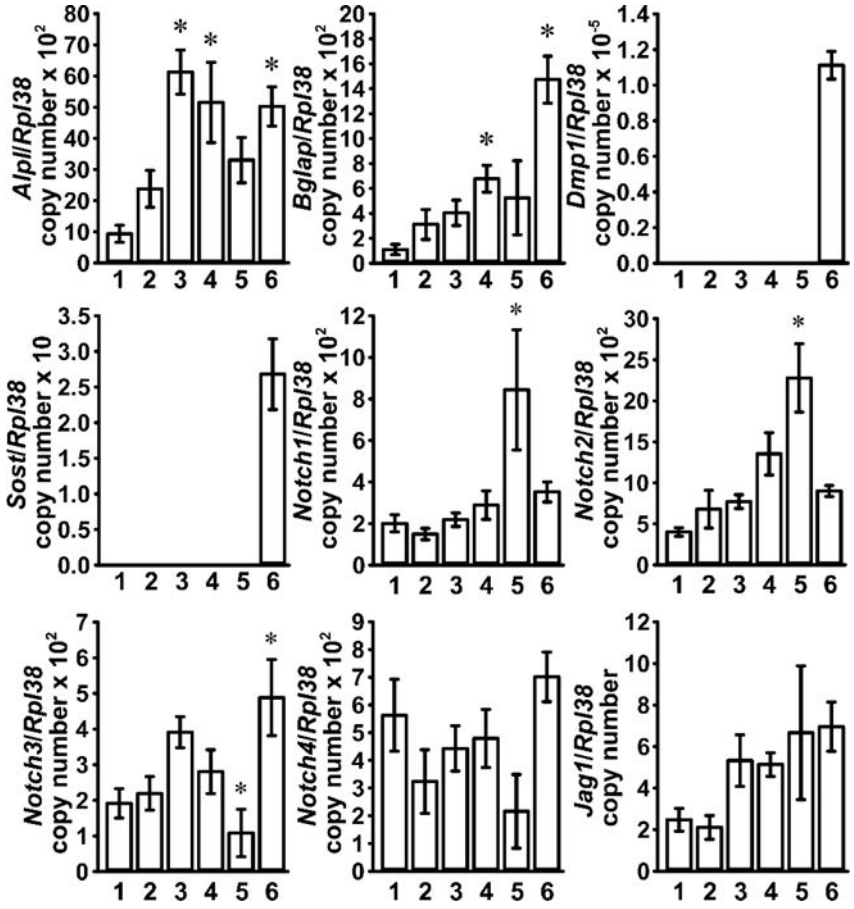

Figure 2. Characterization of Notch expression in osteoblast and osteocyte-enriched cell fractions

Femoral fragments from 6 week old wild-type C57BL/6J mice were exposed sequentially to type-II collagenase (fraction 1, 3 and 4), or EDTA (fraction 2 and 5) and cells collected after each digestion; femoral diaphyses (6) were frozen immediately after the final exposure to EDTA. Total RNA was extracted from cellular fractions and digested bone remnants, and mRNA quantified by qRT-PCR in the presence of specific primers. Data are expressed as *Alpl*, *Bglap*, *Dmp1*, *Sost, Notch1*, *Notch2*, *Notch3*, *Notch4* and *Jag1* copy number, corrected for *Rpl38* expression. Values are means ± SEM; n = 5. *Significantly different from fraction 1, $p < 0.05$ by one-way ANOVA with Holm-Šídák post-hoc analysis.

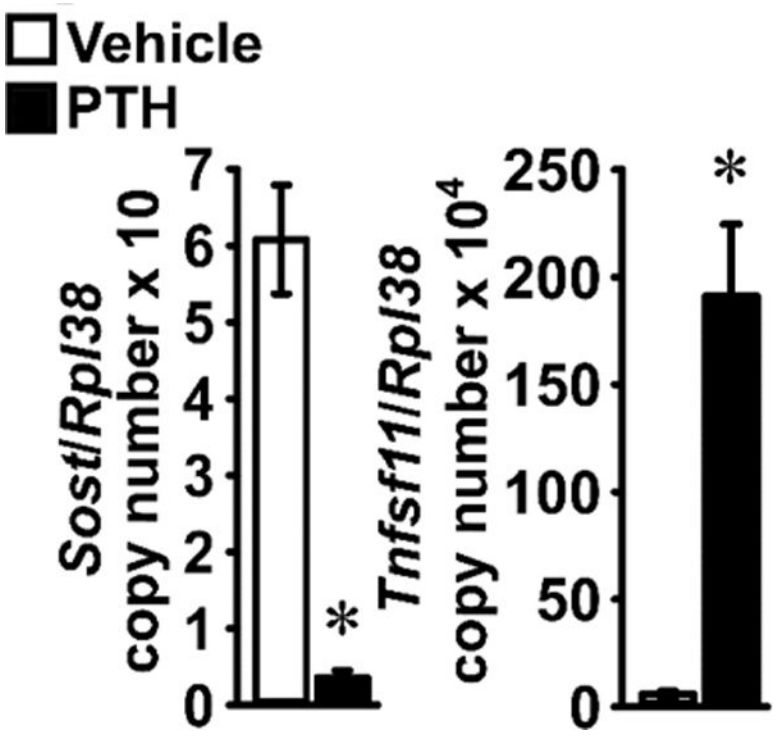

Figure 3. Characterization of osteocyte-enriched cultures

Primary osteocyte-enriched femoral fragments from 6 week old wild-type C57BL/6J mice were cultured for 24 h in the absence of serum and exposed to vehicle (white bars) or to PTH 10 nM (black bars) for 6 h. Total RNA was extracted and mRNA quantified by qRT-PCR in the presence of specific primers. Data are expressed as *Sost* and *Tnfsf11* copy number, corrected for *Rpl38* expression. Values are means ± SEM; n = 6. *Significantly different between vehicle and PTH, $p < 0.05$ by unpaired Student's *t*-test.

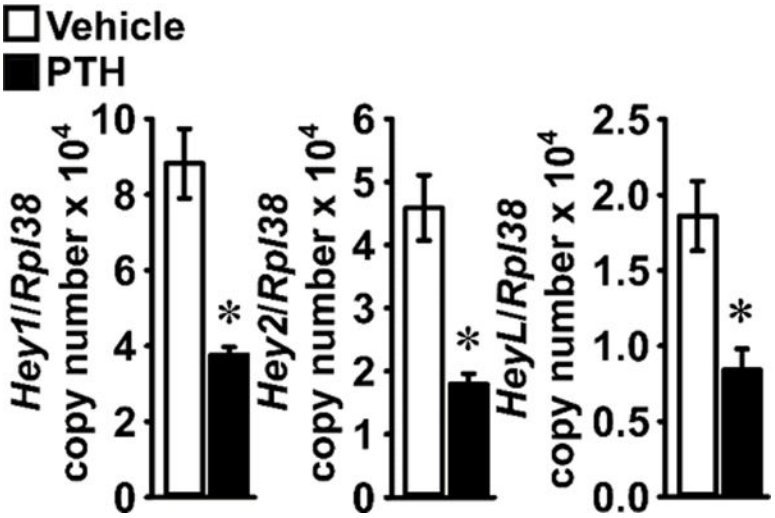

Figure 4. PTH suppresses *Hey1, Hey2* and *HeyL* expression in osteocytes

Primary osteocyte-enriched femoral fragments from 6 week old wild-type C57BL/6J mice were cultured for 24 h in the absence of serum and subsequently exposed to vehicle (white bars) or PTH 10 nM (black bars) for 6 h. Total RNA was extracted and mRNA quantified by qRT-PCR in the presence of specific primers. Data are expressed as *Hey1*, *Hey2* and *HeyL* copy number, corrected for *Rpl38* expression. Values are means ± SEM; n = 6.

*Significantly different between vehicle and PTH, $p < 0.05$ by unpaired Student's *t*-test.

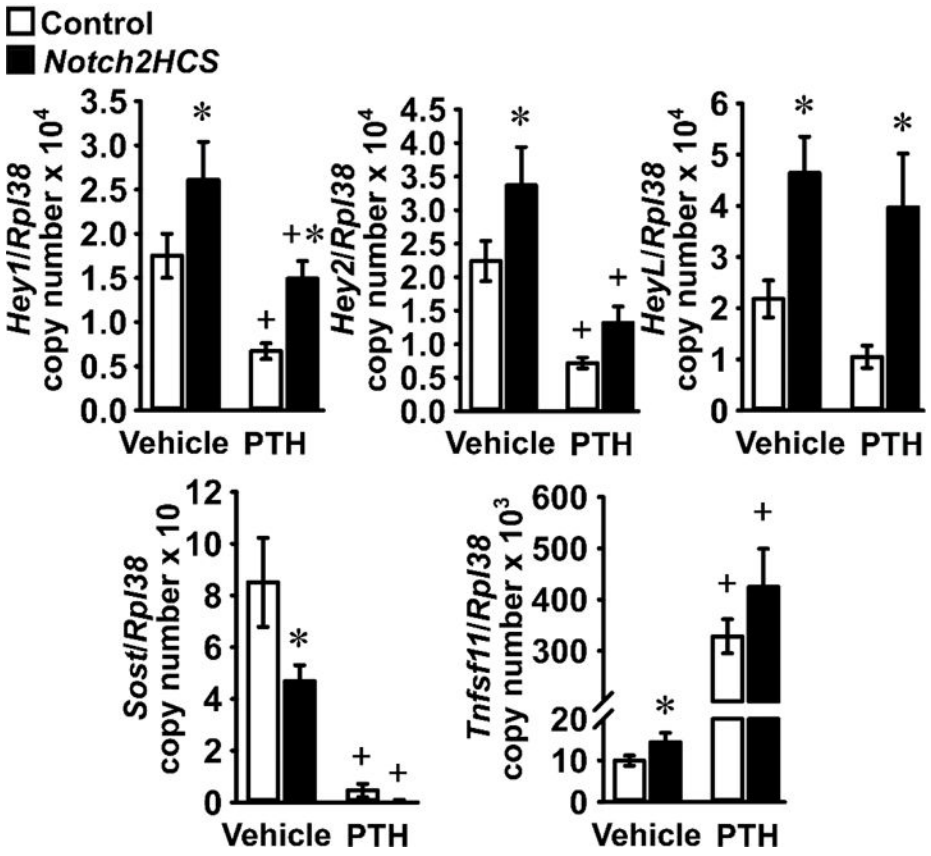

Figure 5. PTH opposes selected effects of *Notch2* gain-of-function in osteocytes

Primary osteocyte-enriched femoral fragments from 7 week old 129SvJ;C57BL/6J wild-type mice (Control, white bars) or *Notch2HCS* littermates (black bars) were cultured for 24 h in the absence of serum and subsequently exposed to vehicle or PTH 10 nM (PTH) for 6 h. Total RNA was extracted and mRNA quantified by qRT-PCR in the presence of specific primers. Data are expressed as *Hey1*, *Hey2*, *HeyL*, *Sost* and *Tnfsf11* copy number, corrected for *Rpl38* expression. Values are means ± SEM; n = 5 – 7. *Significantly different between Control and *Notch2HCS*, $p < 0.05$; $^{+}$significantly different between Vehicle and PTH, $p < 0.05$; two-way ANOVA with Holm-Šídák post-hoc analysis.

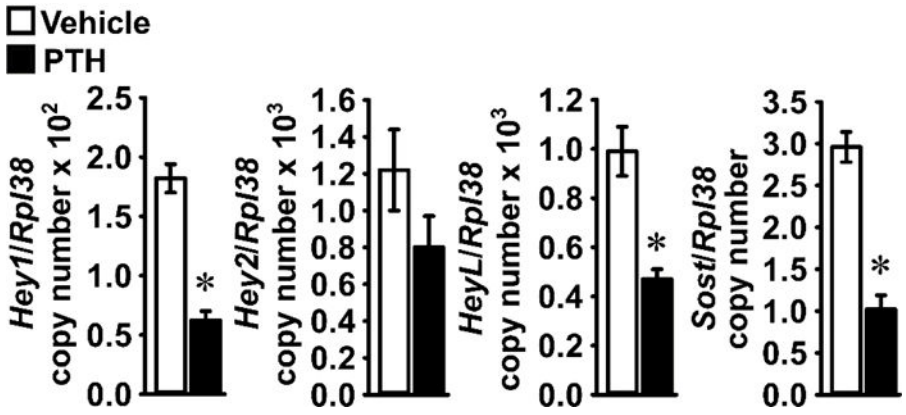

Figure 6. PTH suppresses expression of Notch target genes by bone cells *in vivo*

Seven week-old wild-type C57BL/6J male mice were administered vehicle 5 ml/Kg (white bars) or PTH 80 μg/Kg (black bars) subcutaneously. Mice were sacrificed 3 h after the injections and total RNA extracted from parietal bones and mRNA quantified by qRT-PCR in the presence of specific primers. Data are expressed as *Hey1*, *Hey2*, *HeyL* and *Sost* copy number, corrected for *Rpl38* expression. Values are means ± SEM, n = 4 – 5. *Significantly different between Vehicle and PTH, $p < 0.05$ by unpaired Student's *t*-test.

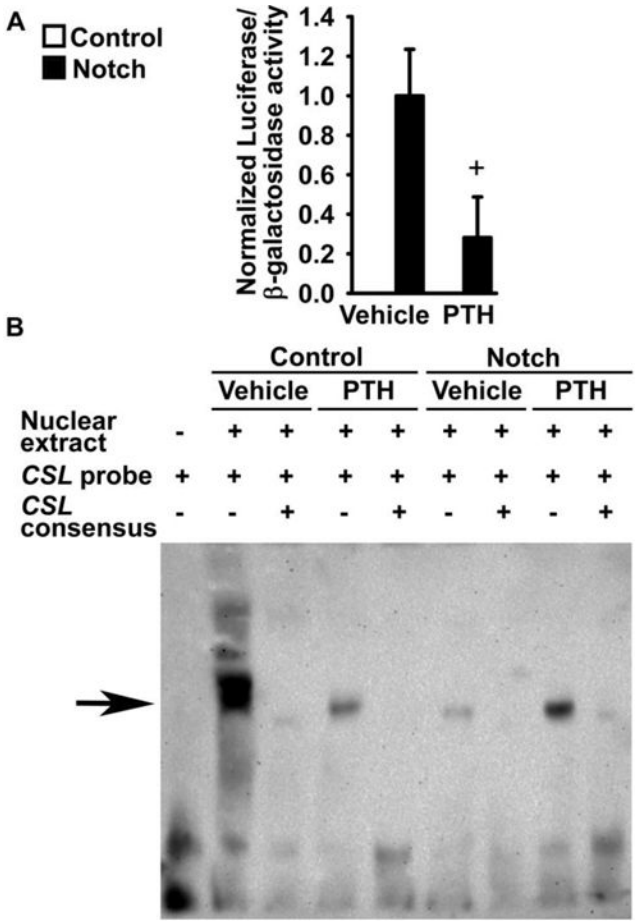

Figure 7. PTH inhibits Rbpjκ-mediated Notch signaling in osteoblasts

Primary osteoblast-enriched cells were harvested from parietal bones of 3 to 5 day old wild-type C57BL/6J mice. In panel A, cells were transiently transfected with pcDNA3.1 (Control) or with pcDNA-NICD (Notch) and co-transfected with the 12xCSL-Luc reporter and a CMV/β-galactosidase expression vector. Cells were cultured for 6 h in the absence of serum, exposed to vehicle or PTH at 10 nM (PTH), and harvested after 24 h. Data represent luciferase/β-galactosidase activity. Values are means ± SEM, n = 6. $^{+}$significantly different between Vehicle and PTH, $p < 0.05$ by unpaired Student's *t*-test. In panels B and C, cells were seeded on BSA (Control) or Dll1 (Notch) coated culture plates. After confluence, cells were cultured for 24 h in the absence of serum and exposed to vehicle or PTH at 10 nM (PTH) for 6 h. In panel B, a biotinylated oligonucleotide containing a *CSL* consensus sequence from the EBNA2 promoter was used. Competition of binding reactions was performed in the presence of unlabeled oligonucleotides containing homologous *CSL* consensus sequences in 200 fold excess. DNA-nuclear protein complexes were resolved by gel electrophoresis, transferred to a nylon membrane, exposed to a streptavidin-horseradish peroxidase conjugate and visualized by chemiluminescence. The arrow indicates the position of DNA protein complexes.

Table 1

Primers for qRT-PCR

Forward (Fwd) and reverse (Rev) primers used for detection of gene expression by qRT-PCR. GenBank accession numbers indicate transcript variants with homologous sequences to the primers.

Gene	Strand	Primer Sequence	GenBank Accession Numbers
Alpl	Fwd Rev	5′-TGGTATGGGCGTCTCCACAGTAACC-3′ 5′-CTTGGAGAGGGCCACAAAGG-3′	NM_007431
Bglap	Fwd Rev	5′-GACTCCGGCGCTACCTTGGGTAAG-3′ 5′-CCCAGCACAACTCCTCCCTA-3′	NM_001037939
Dll1	Fwd Rev	5′-CTCTTCCCCTTGTTCTAAC-3′ 5′-ACAGTCATCCACATTGTC-3′	NM_007865
Dll3	Fwd Rev	5′-TCTATCTTGTCCCTTCTCTATCA-3′ 5′-AATCATTCAGGCTCCATCTC-3′	NM_007866
Dll4	Fwd Rev	5′-TGACAAGAGCTTAGGAGAG-3′ 5′-GCTTCTCACTGTGTAACC-3′	NM_019454
Dmp1	Fwd Rev	5′-CTGTCATTCTCCTTGTGTTC-3′ 5′-TTCAGATTCAGTATTGTGGTATC-3′	NM_016779
Hey1	Fwd Rev	5′-ATCTCAACAACTACGCATCCCAGC-3′ 5′-GTGTGGGTGATGTCCGAAGG-3′	NM_010423
Hey2	Fwd Rev	5′-AGCGAGAACAATTACCCTGGGCAC-3′ 5′-GGTAGTTGTCGGTGAATTGGACCT-3′	NM_013904
HeyL	Fwd Rev	5′-CAGTAGCCTTTCTGAATTGCGAC-3′ 5′-CCCAGCACAACTCCTCCCTA-3′	NM_013905
Jag1	Fwd Rev	5′-TGGGAACTGTTGTGGTGGAGTCCG-3′ 5′-GTGACGCGGGACTGATACTCCT-3′	NM_013822
Jag2	Fwd Rev	5′-AAGGTGGAAACAGTTGT-3′ 5′-CACGGGCACCAACAG-3′	NM_010588
Notch1	Fwd Rev	5′-GTCCCACCCATGACCACTACCCAGTTC-3′ 5′-GGGTGTTGTCCACAGGTGA-3′	NM_008714
Notch2	Fwd Rev	5′-TGACGTTGATGAGTGTATCTCCAAGCC-3′ 5′-GTAGCTGCCCTGAGTGTTGTGG-3′	NM_010928
Notch3	Fwd Rev	5′-CCGATTCTCCTGTCGTTGTCTCC-3′ 5′-TGAACACAGGGCCTGCTGAC-3′	NM_008716
Notch4	Fwd Rev	5′-CCAGCAGACAGACTACGGTGGAC-3′ 5′-GCAGCCAGCATCAAAGGTGT-3′	NM_010929
Rpl38	Fwd Rev	5′-AGAACAAGGATAATGTGAAGTTCAAGGTTC-3′ 5′-CTGCTTCAGCTTCTCTGCCCTTT-3′	NM_001048057 NM_023372 NM_001048058
Sost	Fwd Rev	5′-AGGAATGATGCCACAGAGGTC-3′ 5′-CTGGTTGTTCTCAGGAGGAGGCTC-3′	NM_024449
Tnfsf11	Fwd Rev	5′-TATAGAATCCTGAGACTCCATGAAAAC-3′ 5′-CCCTGAAAGGCTTGTTTCATCC-3′	NM_011613